Cephalosporin Antibiotics Specifically Enhance Conventional Chemotherapy in Nasopharyngeal Cancer

Xiao-Qiong He (hexqcn@aliyun.com)
Kunming Medical University https://orcid.org/0000-0003-4357-2482
Qian Yao
Yunnan Cancer Hospital
Zhong Yu Song
Yunnan Cancer Hospital
Dan Fan
Kunming Medical University
Yu Tong You
Kunming Medical University
Wen Jing Lian
Kunming Medical University
Ling Duan
Kunming Medical University
Zhang Ping Zhou
Kunming Medical University

Research

Keywords: cephalosporin antibiotics, drug repositioning, anticancer drug sensitization, nasopharyngeal carcinoma, conventional chemotherapy, cisplatin, combination therapy

Posted Date: September 8th, 2020

DOI: https://doi.org/10.21203/rs.3.rs-61540/v1

Abstract

Background: Cephalosporin antibiotics can drastically upregulate the expression of HMOX1 in nasopharyngeal carcinoma cells. HMOX1 has dual role in cancer cells, and is involved in chemoresistance. Cephalosporin antibiotics are widely used in the treatment of bacteria infectious diseases in cancer patients. Whether they affect the efficacy of chemotherapy is unknown.

Methods: Comparisons between cefotaxime and the combination of cefotaxime and cisplatin were carried out throughout the study. Cell viability was detected by MTT method. Influence on clone formation of cancer cells was investigated by plate clone formation assay. The in vivo anticancer effect was determined via cancer xenograft in mice. Flow cytometry analysis was used to detect the apoptosis. Microarray gene expression profiling was analyzed using Gene Ontology analysis, and the differential genes were validated by RT-qPCR.

Results: Cefotaxime specifically, selectively and synergistically enhanced the anticancer efficacy of cisplatin in nasopharyngeal carcinoma both in vitro and in vivo without increasing the toxicity, but it inhibited the cytotoxic effects of cisplatin in other cancers. Combination of cefotaxime and cisplatin significantly regulated 5 genes in direction favoring the enhancement of anticancer efficacy; of which, THBS1 and LAPTM5 were upregulated; PPP3CB, STAG1 and NCOA5 were downregulated jointly. HMOX1 contributes to the anticancer efficacy in combination group. Upregulated genes significantly modulated 18 apoptotic pathways, downregulated genes mainly affected assembly of genetic materials.

Conclusion: Cephalosporin antibiotics are excellent and safe sensitizers of conventional chemotherapy in the treatment of nasopharyngeal carcinoma, but should be carefully used in other cancers.

Background

Infectious diseases are the most frequent and life-threatening complications in cancer patients [1, 2]. With the advantages of strong and broad spectrum anti-bacteria activity as well as little toxicity, cephalosporin antibiotics are widely used in the treatment of bacteria infectious diseases. Little is known whether cephalosporin antibiotics affect the efficacy of conventional chemotherapy when cancer patients accept both anticancer and anti-infection treatments at the same time.

In our another study, cephalosporin antibiotics showed highly specific and highly selective anticancer activity in nasopharyngeal carcinoma (NPC) both in vitro and in vivo, mainly via ferroptosis mediated by drastic overexpression of HMOX1. HMOX1 is the top one gene markedly and specifically upregulated by cephalosporins in NPC cells. HMOX1 has dual role in cancer cells [3]. It is commonly regarded as a survival molecule, exerting an important role in cancer progression [4-6]. HMOX1 is frequently overexpressed in a range of cancers [7-9], and is involved in chemoresistance by inhibiting apoptosis and autophagy [10-12]. Ferroptosis is a non-programmed cell death for which key regulators remain unknown [13-15]. However, increasing studies showed that ferroptosis mediated by HMOX1 is a new and prospective chemotherapeutic strategy against cancers [16-18]. The dual role of HMOX1 depends on

different pathological conditions of cancers [3]. Different cancers have different pathological characters because of distinct abnormalities or dysregulations of genes [19]. Cephalosporin antibiotics regulate the expression of HMOX1 and affect the proliferation of cancer cells differently in different cancers in our previous study. We question whether cephalosporin antibiotics affect the efficacy of conventional chemotherapy, and the influence is also different in different cancers, as well as whether HMOX1 contributes to this influence.

Here we find that cephalosporin antibiotics specifically and synergistically enhance the anticancer efficacy of conventional chemotherapeutic drugs in nasopharyngeal carcinoma both in vitro and in vivo, but significantly inhibit the cytotoxic effects of cisplatin on other cancers. Combination of cefotaxime and cisplatin jointly regulates the expression of 5 genes in directions supporting the enhancement of anticancer efficacy, and overexpression of HMOX1 contributed to the specific anticancer efficacy in nasopharyngeal carcinoma.

Methods

Samples

Cefotaxime sodium (COS), cefmetazole sodium (CMS), cisplatin (DDP) and 5-fluorouracil (5-Fu) were purchased from hospitals and freshly dissolved into PBS for use (stored in shadow at 4℃). The final concentrations of COS and CMS in complete medium were 25, 50, 100, 200 and 400 μg/ml; cisplatin were 0.5, 1.0, 2.0, 3.0 and 4.0 μg/ml; 5-Fu were 1, 2, 4, 8 and 16 μg/ml in the in vitro study. The doses of cefotaxime sodium used in the in vivo xenograft mouse study were 200 mg/kg; DDP was 2 mg/kg.

Cell lines and cell culture

Human non-small cell lung carcinoma (A-549), Xuanwei lung carcinoma (XWLC-05), hepatocellular carcinoma (HepG2), colorectal carcinoma (HCT-116), stomach gastric carcinoma (SGC-7901), nasopharyngeal carcinoma (CNE2), neuroglioma (U-251), breast carcinoma (MCF-7) and human normal epithelia cell of vein (ECV-304) cell lines were friendly provided by Institute of Yunnan Tumor stocks, which were purchased from Cell Bank of Kunming Animal Institute, China Academy of Science. All cell lines were cultured in DMEM/F12 medium (Hyclone) supplemented with 10% fetal bovine serum (FBS) (complete medium) (free of antibiotics) at 37℃ in a 5% CO_2, humidified incubator.

Mice

6-8 weeks age male balb/c nude mice were purchased from Beijing Vital River Laboratory Animal Technology Co., Ltd. Mice were fed in the temperature- and humidity- controlled Specific Pathogen Free Animal Facility of Kunming Medical University, with a 12-hr light-dark cycle. Mice were fed autoclaved distilled water and autoclaved rodent chow. Animal work described in this manuscript has been approved by the Ethical Committee of Kunming Medical University, China. All methods were carried out in accordance with relevant guidelines and regulations.

Cell viability assay

Cellular viability was determined by MTT assay. Cells were collected when they were cultured in the incubator for 72h and covered about 90% of the flask bottom. 200 μl complete DMEM/F12 medium with applicable cell number were seeded into wells of 96-well plates and incubated overnight. The following day, the original medium was gently removed by injector, 200 μl new complete medium containing different concentrations of samples was added into each well according to experiment design. 8 replicate wells were done for each concentration. Then, cells were incubated for 72 hrs. After removing the medium, 200 μl new complete medium containing 10% MTT（5 mg/ml）was added into each well. Plates were incubated for another 4 hours. After carefully removing the MTT medium, 150 μl DMSO was added into each well. Plates were then shaken in the shadow for 10 minutes. OD (optical density) values were determined by microplate reader at 490 nm. Deleting the highest and the lowest OD value in each group, 6 OD values in each group were remained for statistical analysis. Inhibition rates of cell viability were calculated using the following formula:

Inhibition rate = (Ac - Ad) / Ac × 100%.

Ac: the corrected absorbance (OD value) of the vehicle control group.

Ad: the corrected absorbance (OD value) of the drug group.

Corrected absorbance = OD value of sample group – OD value of blank control group

Plate clone formation assay

1,000 cells were seeded into each well of the 6-well culture plate. Cells were adhered overnight in the incubator. On the next day, after the medium in the wells was removed, 2 ml new medium containing different concentrations of drugs was added into each well, and 3 replicate wells were done in each group. Plates were further incubated for 14 days, during the period the medium was renewed at an interval of 5, 4, 3 days and cell state was observed. On the 14^{th} day, each well was washed with 2 ml 0.01M PBS for one time, and then cells were fixed with 5% paraformaldehyde for 15 minutes. Discarding the paraformaldehyde, each well was washed with 2 ml 0.01M PBS for one time, and stained with 0.5 ml of 0.5% crystalviolet for 10 minutes, and then washed once with 2 ml 0.01M PBS. At last, the pictures were acquired with a camera, and the number of clones was counted.

Inhibition rate = (Nc - Nd) / Nc × 100%.

Nc: the clone number of the vehicle control group.

Nd: the clone number of the drug group.

Detection of apoptosis by flow cytometer

Experimental groups: solvent control group (PBS), cisplatin group (DDP, 2 μg/ml), COS group (200 μg/ml), COS+DDP group. Annex-V FITC/PI kit was used for apoptosis detection. Cells were seeded into 25 cm^2 flasks and treated with samples as described in the cell viability assay. At the end, all cells including the cells died and floating in the medium were collected. Cells then were treated according to the protocol of the kit: each sample was added 0.4 ml binding buffer, resuspended, then added 5 μl Annex-V/FITC and mixed to be stained in ice for 15 minutes. Then 10 μl PI was added into each sample to incubate for 30 minutes at room temperature in dark. And then samples were detected by a flow cytometer according to standard protocol, in which flow cytometer would collect more than 10,000 events in each sample. During the process, the live and normal cells were not stained with Annexin-V/FITC and PI (Q3), the early apoptotic cells were only stained with Annexin-V/FITC (Q4), and the late apoptotic cells were stained with both Annexin-V/FITC and PI (Q2), and the necrotic cells and mechanically damaged cells were only stained with PI (Q1).

Tumor growth study in cancer xenograft model

Nasopharyngeal carcinoma CNE2 cells were collected during logarithmic stage and rinsed with PBS for two times, then resuspended into density of 4×10^7 cells/ml using fresh DMEM/F-12 medium free of FBS and antibiotics. Each mouse was inoculated 0.1ml cell suspension subcutaneously on the right side flank. Mice were fed autoclaved distilled water and autoclaved rodent chow. 8 days later after cell inoculation, tumor-bearing mice were used for in vivo anticancer study when the average tumor volume was around 200 mm^3. 24 tumor-bearing mice were randomly allocated into 4 groups (6 tumor-bearing mice per group): vehicle control group (NS, neutral saline), COS group (200 mg/kg), DDP group (2 mg/kg) and combination group (COS+DDP). Mice were injected intraperitoneally 0.10 ml/10g b.w sample (mice in the vehicle control group were injected the same volume of neutral saline) each time for each mouse, 2 times a day at an interval of 6 hours (9:00 Am and 3:00 Pm). DDP was injected one time a day at one day interval in the morning. Body weight and tumor volume of each mouse were measured every 4 days. Mice were sacrificed at 12^{th} day of drug treatment. Tumors were carefully isolated and weighed. Auto-reading caliper was used to measure the size of tumor. Tumor volume was calculated using the follow formula.

Tumor volume (TV) = $(a \times b^2) / 2$, “a” is the longitude range; “b” is the short diameter.

Relative tumor volume (RTV) = V_T / V_0, V_0 is the tumor volume measured when grouping, V_T is the tumor volume measured at each experiment time point.

Relative proliferation ratio (RPR) = $(T_{RTV} / C_{RTV}) \times 100\%$ T_{RTV} is the relative tumor volume of the drug group, C_{RTV} is the relative tumor volume of the solvent control group.

Microarray gene expression profiling

CNE2 cells were treated with neutral saline (NS), COS (200 μg/ml), DDP group (2 μg/ml) and COS+DDP respectively for 48h. After washed with cooled PBS for 2 times, the total RNA was rapidly extracted from the cells with Trizol and then samples were stored in -80℃ fridge and be sent to Shanghai Qi Ming

Biological Information LTD for microarray gene expression profiling analysis using Affymetrix GeneChip® Human Transcriptome Array 2.0 after quality examination of sample RNA and gene chip. Gene chip data was pre-analyzed using RMA (Robust Multiarray Average) method. Gene expression analyses was performed using GO (Gene Ontology) and KEGG (Kyoto Encyclopedia of Genes and Genomes) by experts using Gene Cloud Biotechnology Information (GCBI) software. Genes were filtered using microarray fold change (logFC ≥ ±1.00). The biological process, molecular function, cell component, signal networks, signaling pathway network, and KEGG pathway that were enriched / modulated by samples in CNE2 cell lines were analyzed. The raw microarray data files were submitted to Gene-Cloud of Biotechnology Information (GCBI) repository. The microarray data was validated by profiling the expression of genes through quantitative reverse transcription PCR (RT-qPCR).

Quantitative reverse transcription PCR (RT-qPCR)

The microarray data was validated by profiling the expression of genes through quantitative reverse transcription PCR (RT-qPCR). Each data point presented for the quantitative PCR assay was derived from three biological replicates (BR). Total RNA from each BR was reversed transcribed and the cDNA from each BR was used as a template for the qPCR. Seven genes were selected to validate the microarray data, comprising of four upregulated differential genes (THBS1, SAMD9, PI3 and LAPTM5) and three downregulated differential genes (PPP3CB, STAG1 and NCOA5). Primers were designed according to the relevant target gene sequences published by GenBank. Table 5 lists the primers used for the RT-qPCR. Shanghai Qi Ming Biological Information LTD synthesized the primers.

After CNE2 cells were treated with drugs for 48 h, the total RNA was extracted with Trizol. The extracted total RNA was re-transcribed into cDNA. Finally, the fluorescence quantitative PCR reaction was carried out in a fluorescence quantitative PCR instrument. The thermocycling conditions were 95°C for 30 s, followed by 40 cycles of 95°C for 10 s and 60°C for 30 s. GAPDH was selected as the internal control gene to normalize the gene expression data. Relative quantification of the target genes was calculated by comparative $2^{-\triangle\triangle CT}$ method.

Statistical analysis

The data from three independent groups or above was analyzed by one-way ANOVA. Statistical comparisons were carried out by independent *t*-test. Data was represented as mean ± SEM in duplicate assays and analyzed using SPSS statistical software version 21.0. $^{*/\#}$ meant P<0.05, $^{**/\#\#}$ meant P<0.01, $^{***/\#\#\#}$ meant P<0.001. The acceptable level for statistical significance was $P < 0.05$.

Results

Cefotaxime specifically enhances the anti-proliferation efficacy of cisplatin in NPC cells

Cefotaxime sodium (COS) showed highly specific and highly selective anti-proliferation activity in CNE2 via ferroptosis in another study (Fig. S1A). Cisplatin (DDP) is a broad spectrum anticancer drug which is

widely used in the treatment of cancers. In present study, DDP significantly reduced the cellular viability of all cells in a concentration-dependent manner (Fig. 1A-1J, NO). After adding the same concentration of cefotaxime into medium (200 μg/ml), the optical density (OD) values in CNE2 cells at each concentration of DDP was significantly and synergistically reduced (Fig. 1A), while OD values in other cancers were significantly and antagonistically increased (Fig. 1B-1H). Cefotaxime showed contrary effects on the anti-proliferation efficacy of DDP, and the influence varied in different cancers. The inhibition rates of cell viability in CNE2 in COS+DDP group were significantly higher than those in DDP group at each DDP concentration (Fig. 1J).

In addition to DDP, cefotaxime and cefmetazole also significantly enhanced the anti-proliferation efficacy of 5-fluorouracil (5-Fu) in CNE2 in vitro (Fig. S1B).

Cefotaxime does not promote the cytotoxicity of DDP in normal cells

One of the most common toxic side effects in conventional chemotherapy is the damage of vascular. Human epithelial cell of vein ECV304 was used to assess the cytotoxicity in normal cells. Results showed that the cytotoxicity in ECV304 cells treated by DDP and COS+DDP was very close at each DDP concentration, and no significant difference was found at the DDP concentration of 2 μg/ml (Fig. 1I). Furthermore, when we analyzed the anti-proliferation efficacy of DDP in CNE2 and ECV304 according to the medium containing COS or not, we found that DDP showed much stronger cytotoxicity in ECV-304 cells than in CNE2 cells (Fig. 1K) when the medium contained no cefotaxime; however, the situation was inversed when the medium contained cefotaxime, in which DDP showed much stronger cytotoxicity in CNE2 cells than in ECV-304 cells (Fig. 1L). Cephalosporin antibiotics selectively enhanced the anti-proliferation efficacy of DDP in NPC cells without enhancing the cytotoxic efficacy of DDP in normal vascular cells correspondingly.

Cefotaxime reduces clone formation of CNE2 and HepG2 cells treated by DDP

The effects of DDP and COS+DDP on the clone formation of two cancer cell lines were investigated. The clone number decreased with the increasing of DDP concentration in both HepG2 (Fig. 2A) and CNE2 (Fig. 2C). When adding 50 or 100 μg/ml of cefotaxime into medium, the clone formation was further inhibited in both cell lines (Fig. 2B, 2D). With the increasing of COS concentration, the inhibition rates of clone formation in HepG2 (Fig. 2E) and CNE2 (Fig. 2F) significantly increased at the same DDP concentration. HepG2 was more sensitive to DDP than CNE2 no matter the medium containing cefotaxime or not. Cells were completely killed and no clone was formed at the DDP concentration of 0.8 and 1.6 μg/ml in HepG2, or 1.6μg/ml in CNE2 when medium containing 100 μg/ml of COS; and at 1.6 μg/ml of DDP in HepG2 when medium containing 50 μg/ml of COS. Cefotaxime greatly and significantly promoted the anticancer efficacy of DDP in both cancers in a concentration-dependent manner when they were concomitantly used for a long period (14 days).

Cefotaxime enhances the anticancer efficacy of DDP in NPC xenograft mouse model without increasing toxic effect

The combination anticancer effect of COS and DDP in vivo was determined via NPC xenograft in balb/c nude mice. The average original tumor volumes (TV0) in each group before drug administration were close and showed no statistically significant difference (Fig. 3A). NPC xenograft grew rapidly in neutral saline control group (NS), so the animal experiment had to be ended at the third examination point (after 12 days of drug administration).

Mice were injected intraperitoneally neutral saline (NS), COS (200 mg/kg), DDP (2 mg/kg), and combination of COS and DDP (COS+DDP) respectively. The relative tumor volume (RTV) (Fig. 3B) and the relative proliferation rate (RPR) of tumor (Fig. 3C) in combination group were markedly less than those in NS, COS, and DDP groups throughout the study. RTV in combination group was significantly less than that in NS group at day 8^{th} and 12^{th}, in COS group at day 12^{th} (Fig. 3B). At the end of the experiment, the relative tumor volume (RTV3) in combination group was only 3.66 folds of the tumor volume before drug administration (TV0), which was significantly less than 12.11 folds in NS group and 7.48 folds in COS group, and markedly less than 6.63 folds in DDP group respectively (Fig. 3D). The relative proliferation rate (RPR3) of NPC tumor in combination group were only 30.26%, which were also markedly less than 100%, 54.72% and 61.76% in NS, DDP and COS groups respectively. Tumor volume (TV) in combination group increased very slowly throughout the study, and tumor growth was greatly and significantly retarded. The average tumor weight (TW) in combination group was only 0.81g, which was also significantly less than 2.01g in NS group, 1.65g in COS group and 1.25g in DDP group (Fig. 3E). Results of TV, RTV, RPR and TW were consistent with each other; which confirmed that combination of COS and DDP significantly and synergistically inhibited the growth of NPC xenograft in mice. Compared with neutral saline control group, the body weights of mice in DDP group and combination group significantly dropped at the end of the study (Fig. 3F). However the body weights in DDP group and combination group were very close at each time point and had no significant difference between them throughout the study. The drop of body weight in combination group was obviously resulted from the toxicity of DDP. Cefotaxime significantly enhanced the anticancer efficacy of DDP in NPC in mice without enhancing the toxic effect of DDP.

Cefotaxime specifically promotes the apoptosis in CNE2 cells treated by DDP

Flow cytometry (FCM) analysis was used to detect the apoptosis in CNE2 (Fig. 4A-4E), A-549, HepG2 and ECV-304 cells (Fig. 4F) treated by COS (100 μg/ml), DDP (2 μg/ml) and COS+DDP respectively. Because of the time-delayed effect of COS in CNE2 cells as we found in another study, the apoptosis was detected after CNE2 cells were treated with drugs for 72 hours. Early apoptosis rate (EA, Q4), late apoptosis rate (LA, Q2) and total death rate (TD, Q1+Q2+Q4) in CNE2 cells were 27.26%, 24.94% and 83.35% in combination group; 19.30%, 30.26% and 70.99% in COS group; and 34.50%, 23.00% and 66.59% in DDP group (Fig. 4E). TD in combination group (83.35%) was markedly higher than that in COS (70.99%) or DDP group (66.59%). Combination of COS and DDP jointly promoted apoptosis induction in CNE2 cells. Result of apoptosis in CNE2 cells was consistent with that of cell viability (Fig. 1A) and clone formation (Fig. 2F). Enhancement of apoptosis is the chemotherapeutic strategy of COS+DDP against NPC.

However, contrarily, after 48 hours of drug intervention, the total death rates in A-549, HepG2 and ECV-304 in the combination group were less than those induced by DDP alone (Fig. 4F). COS reduced the apoptosis in these cell lines induced by DDP, which was also consistent with the results of cell viability that COS significantly inhibited the anti-proliferation efficacy of DDP in cancers except CNE2 (Fig. 1B-1H). The total death rate of ECV-304 in combination group (23.20%) was close to that in DDP group (24.32%), which also proved that COS did not promote the cytotoxic effect of DDP on normal vascular cells (Fig. 1I).

Combination of cefotaxime and DDP regulates genes and pathways in direction favoring the enhancement of anticancer activity in CNE2 cells

Gene expression in CNE2 cells treated by COS, DDP and COS+DDP for 48 hours was detected by microarray assay and analyzed using GO (Gene Ontology) analysis with a cut-off fold change (FC) value of logFC $\geq \pm 1.00$. COS regulated differential expression of 31 coding genes (7 genes upregulated), DDP regulated differential expression of 178 coding genes (40 genes upregulated), and COS+DDP regulated differential expression of 120 coding genes (40 genes upregulated). The differential coding genes favoring anticancer activity and jointly upregulated in the combination group were THBS1, PI3 and SAMD9 (Fig. 5A); and the differential coding genes jointly downregulated in the combination group were PPP3CB, STAG1 and NCOA5 (Fig. 5B). Expressions of these differential coding genes in combination group were jointly enhanced or decreased in direction supporting the enhancement of anticancer efficacy. LogFC of HMOX1 was 0.3462, 2.3472 and 2.1126 in DDP group, COS group and combination group respectively. Although HMOX1 was not jointly enhanced in combination group, it was still greatly overexpressed as that in COS group. Ferroptosis mediated by overexpression of HMOX1 in NPC cells has been proved to be the specific and selective chemotherapeutic strategy of cephalosporin antibiotics against NPC in another study. Therefore, HMOX1 contributed to the anticancer efficacy in CNE2 in combination group, but did not contribute to the enhancement of anticancer efficacy. The logFC of LAPTM5 was -0.3822, 1.5632 and 1.4721 in COS group, DDP group and COS+DDP group respectively. LAPTM5 was not jointly upregulated in combination group, but it still overexpressed in combination group.

Combination of COS and DDP significantly modulated canonical pathways, which are associated with apoptosis, cell proliferation, cell cycle, DNA replication, etc. There were 18 significantly regulated apoptotic pathways (Biological Pathway in GO-term) mediated by the upregulated differential coding genes; and no significantly regulated apoptotic pathways mediated by the downregulated differential coding genes in combination group; compared with 23 and 11 apoptotic pathways in COS group, 6 and 2 in DDP group respectively (Table S1, S2). 15 significantly regulated apoptotic pathways in combination group were also regulated by COS, and 2 pathways regulated by DDP. 2 new significantly regulated apoptotic pathways (Go: 0043652 and 1902043) appeared in combination group. HMOX1 and THBS1 were overlapped in 12 and 14 apoptotic pathways, and THBS1 was the only overlapped gene in the 2 new apoptotic pathways. Extrinsic apoptotic signaling pathway (Go: 2001236) was the only apoptotic pathway which was significantly regulated by COS, DDP and COS+DDP at the same time; and THBS1

and HMOX1 were also overlapped in this pathway. HMOX1 and THBS1 were the critical genes associated with apoptosis induction in CNE2 cells. LogFC of THBS1 was only 0.4647 and 0.9607 in COS group and DDP group respectively, it was jointly enhanced to 1.2644 in combination group. THBS1 contributed to the enhancement of apoptosis in combination group.

KEGG (Kyoto Encyclopedia of Genes and Genomes) enriched 5 up-gene-goPathways (Table S3) and 3 down-gene-goPathways (Table S4) significantly in combination group. Out of them, p53 signaling pathway (hsa04115) is closely associated with cell proliferation, apoptosis and cell cycle. GO analysis showed the top ten biological pathways, cell components and molecular functions (GO-term) significantly regulated in combination group (Fig. 6). Modulation of bindings (such as chromatin DNA binding, nucleosomal DNA binding and nucleosome binding) was the important Molecular Function in GO-Pathway analysis. 9 out of the top ten biological pathways in the Downgene-Sig-Go were associated with regulation of genetic materials.

Validation of microarray data by RT-qPCR

The validation was performed by measuring the expression of 7 differential coding genes (PI3, LAPTM5, THBS1, SAMDP, PPP3CB, NCOA5 and STAG1; 4 upregulated, 3 downregulated), including the 6 genes jointly regulated in microarray data in combination group in figure 5A and 5B through RT-qPCR. These genes were selected based on their important roles in anticancer processes, as well as whether they were the differential genes in DDP group or COS+DDP group in microarray data.

The relative expression level (REL) of the 7 validated genes in RT-qPCR techniques are shown in figure 5C (upregulated genes) and 5D (downregulated genes). RT-qPCR results demonstrated that, out of the 7 genes, the expressions of 5 coding genes (THBS1, LAPTM5, and PPP3CB, STAG1, NCOA5) were jointly regulated in direction supporting the enhancement of anticancer efficacy in combination group. The expression of THBS1, PPP3CB, STAG1 and NCOA5 agreed with microarray data in figure 5. They are the chemotherapeutic targets in combination group. The REL of SAMD9 and PI3 were 4.44 and 6.11 in combination group. SAMD9 and PI3 were overexpressed as they were in DDP group, but their expressions were not jointly promoted in combination group. SAMD9 and PI3 contributed to the anticancer activity in combination group, but did not contribute to the enhancement of anticancer efficacy in CNE2.

Discussion

Infectious diseases are the most frequent and life-threatening complications in cancer patients [20, 21]. Antibiotics are frequently used in cancer patients both in hospital and in family for the treatment or prevention of infectious diseases [22, 23]. However, little is known about the influences of antibiotics on the efficacy of conventional chemotherapy when cancer patients accept anticancer drugs and antibiotics at the same time.

Cephalosporin antibiotics disrupt the synthesis of the peptidoglycan layer of bacterial cell walls by inhibition of beta-lactamase activity, which causes the walls to break down and eventually the bacteria

die [24, 25]. Because of broad spectrum anti-bacteria activity and little toxicity, cephalosporin antibiotics are widely used for the treatment of bacteria infectious diseases in cancer patients. Whether cephalosporin antibiotics interfere with the efficacy of conventional chemotherapy is not known by clinicians and patients.

Present study revealed that cephalosporin antibiotics significantly affect the anticancer efficacy of conventional chemotherapeutic drugs. Cephalosporin antibiotics mediate protective or detrimental effects depending on the pathological conditions of cancers. Cephalosporin antibiotics synergistically enhanced the anticancer efficacy of conventional chemotherapy in NPC without increasing the toxicity both in vitro and in vivo; in addition to that cephalosporin antibiotics themselves showed specific and selective anticancer effects on NPC. Cephalosporin antibiotics are the best choice of antibiotics in NPC patients which not only benefit the treatment of infectious diseases, but also benefit the treatment of NPC at the same time. However, our study also revealed that cephalosporin antibiotics significantly reduced the anticancer efficacy of conventional chemotherapeutic drugs in other cancers. Therefore cephalosporin antibiotics should be carefully used in the treatment of infectious diseases in other cancer patients when patients are accepting conventional chemotherapy at the same time.

THBS1, LAPTM5, PPP3CB, STAG1 and NCOA5 were the differential genes regulated by combination of cefotaxime and cisplatin in CNE2 cells in both microarray gene expression profile and RT-qPCR analysis. They were jointly regulated in direction supporting the enhancement of anticancer activity. These genes are the combination chemotherapeutic targets against NPC. Although expressions of HMOX1, PI3 and SAMD9 were not jointly upregulated in combination group, their overexpression in combination group contributed to the anticancer efficacy in CNE2.

Thrombospondin 1 (THBS1) is known to be antiangiogenic. THBS1 functions as a tumor suppressor in lung adenocarcinoma [26]. Deregulation of THBS1 promotes the migration, invasion, and progression of bladder cancer [27]. THBS1 expression was jointly and markedly enhanced in COS+DDP group. THBS1 was the most frequently overlapped gene in the significantly modulated pathways. It was involved in 174 of the 456 significantly regulated pathways, especially in 14 of the 18 significantly regulated apoptotic pathways in combination group. THBS1 was overlapped in p53 signaling pathway (hsa04115) and ECM-receptor interaction pathway (hsa04512) significantly enriched in KEGG. THBS1 was the critical gene contributed to the enhancement of apoptosis and anticancer efficacy in combination group.

Lysosomal-associated protein multispanning transmembrane 5 (LAPTM5) is a membrane protein that localizes to intracellular vesicles. LAPTM5 mRNA level is frequently decreased in various cancer cell lines [28]. Overexpression of LAPTM5 in cancer cells induces lysosomal cell death due to lysosomal destabilization [29]. Low expression in patients was significantly correlated with poor prognosis. Inactivation of LAPTM5 may contribute to tumorigenesis in a subset of human cancers [30]. Relative expression levels (REL) in RT-qPCR were 1.07, 5.05 and 5.86 in COS, DDP and COS+DDP group respectively. Expression level of LAPTM5 was jointly enhanced by the combination of COS and DDP, which favors the enhancement of anticancer activity.

The Sterile Alpha Motif Domain-containing 9 (SAMD9) gene is expressed at a lower level in lots of cancers [31] It has been reported as a potent tumor suppressor gene that inhibits tumorigenesis and progression of lung cancer [32]. Knockdown of SAMD9 expression increased the invasion, migration and proliferation of cancer cells in vitro and overexpression of SAMD9 suppressed proliferation and invasion in A549 cells [33]. Although expression of SAMD9 was not jointly enhanced in combination group, it was still greatly overexpressed (REL=4.44). SAMD9 was associated with fusion of intracellular vesicle, and LAPTM5 localizes to intracellular vesicles. Whether the overexpression of LAPTM5 and SAMD9 in combination group synergistically works and favors the enhancement of anticancer efficacy by lysosomal cell death via lysosomal destabilization is warranted for further study.

Elafin (PI3) is an elastase-specific inhibitor. It is transcriptionally down-regulated in most tumor cell lines [34]. Induction of elafin, leads to inhibition of human breast cancer cell viability and predicts survival in breast cancer patients [35]. Elafin plays a direct role in the suppression of tumors through inhibition of elastase [36]. Elafin elicits pro-apoptotic effects in melanoma cells but not in normal melanocytes. Elafin induces apoptosis in melanoma cells through a p53-dependent intrinsic apoptotic pathway, and repression of elafin expression in melanoma may contribute to disease progression [37]. In this article, although expression of PI3 was not jointly enhanced, PI3 was markedly overexpressed in combination group. REL of PI3 in combination group (6.11) was very close to that in DDP group (6.19). High expression level of PI3 in combination group was obviously resulted from DDP intervention, and was not affected by cephalosporin antibiotics. Although PI3 did not contribute to the enhancement of anticancer efficacy in combination group, PI3 was still an important chemotherapeutic target against NPC.

High PPP3CB expression was an independent indicator predicting poor prognosis of neuroblastoma (NB) [38]. PPP3CB contributes to poor prognosis through activating nuclear factor of activated T-cells signaling in NB. Overexpression of PPP3CB promoted cell growth, but PPP3CB knockdown decreased cell growth in NB cells. In vitro and in vivo experiments indicated that the loss of PPP3CB suppressed tumor growth [39]. In present study, PPP3CB was jointly and synergistically downregulated by the combination of COS and DDP in CNE2 cells. Decreased expression of PPP3CB in combination group enhanced the anticancer efficacy.

STAG1 and STAG2 support sister chromatid cohesion to redundantly ensure cell survival [40]. STAG2 is a core component of cohesion and a tumor suppressor. STAG1 is the paralog of STAG2. Blocking of STAG1 significantly reduces cell proliferation. STAG1 is a promising therapeutic target in cancers with inactivating alterations of STAG2 [41]. By inhibiting STAG1, holds the promise for the development of selective therapeutics. The REL of STAG1 was 0.880, 0.872 and 0.302 in COS, DDP and COS+DDP group respectively. STAG1 was jointly and synergistically downregulated by the combination of cisplatin and cefotaxime. STAG1 is an important combination chemotherapeutic target. Much lower expression of STAG1 contributes to the synergistic anticancer effects.

Nuclear receptor coactivator 5 (NCOA5) is known to modulate ERα-mediated transcription and has been found to be involved in the progression of several malignancies. NCOA5 overexpression was significantly

correlated with progression and prognosis in luminal breast cancer. Breast cancer patients with high NCOA5 expression had significantly lower overall survival. [42]. Expression of NCOA5 in human colorectal carcinoma (CRC) tissues was notably higher than that in adjacent tissues. Knockdown of NCOA5 markedly suppressed proliferation, migration and invasion of CRC cells. Silencing of NCOA5 also inhibited in vivo growth of CRC xenograft tumors. Overexpression of NCOA5 promoted CRC cell proliferation, migration and invasion [43]. LogFC of NCOA5 in microarray array were -0.48, -0.61 and -1.02; REL in RT-qPCR were 0.68, 0.53 and 0.37 in COS, DDP and COS+DDP group respectively. Expression of NCOA5 was jointly downregulated in COS+DDP group and lower expression of NCOA5 in CNE2 cells contributed to the enhancement of anticancer efficacy.

HMOX1 was the top one gene markedly upregulated by COS in CNE2 cells in a concentration-dependent manner. LogFC of HMOX1 were 1.07, 2.35 and 4.41 by microarray gene expression profile; REL were 8.28, 46.10 and 250.73 by RT-qPCR at COS concentrations of 50, 100 and 200μg/ml. HMOX1 is a main chemotherapeutic target of COS against NPC via ferroptosis in another study. In present study, expression level of HMOX1 in COS+DDP group was close to that in COS group. HMOX1 did not contribute to the enhancement of anticancer efficacy, but overexpression of HMOX1 was still the specific and selective chemotherapeutic target in CNE2 cells in combination group.

Although ferroptosis mediated by HMOX1 activation creates a new chemotherapeutic strategy for cancer treatment, overexpression of HMOX1 was found in a range of cancers. HMOX1 is usually considered a survival molecular. The role of HMOX1 depends on the expression level and the pathological condition of cancers. Excessive activation of HMOX1 leads to ROS overload and death of cancer cells [44-46]. However, HMOX1 exerts a cytoprotective effect by neutralizing ROS when it is activated moderately. In this study, cefotaxime synergistically enhanced the anticancer efficacy of DDP in NPC both in vitro and in vivo, but significantly reduced the anti-proliferation efficacy of DDP in other cancers contrarily. Ferroptosis mediated by drastic overexpression of HMOX1 in NPC cells was the main and the specific chemotherapeutic strategy of cephalosporin antibiotics against NPC. Whether HMOX1 was moderately activated by cefotaxime and consequentially neutralized ROS in other cancers which contributed to the contrary effects is warranted for further study.

Conclusion

In summary, concomitant use of cephalosporin antibiotics significantly alters the chemotherapeutic efficacy of chemotherapeutic drugs and cancer progression. That cephalosporin antibiotics mediate protective or detrimental effects depends on the pathological condition of cancers. Cephalosporin antibiotics are excellent and safe sensitizers of conventional chemotherapy in the treatment of nasopharyngeal carcinoma, but should be carefully used in other cancer patients. Our discovery provides insight into the influence of cephalosporin antibiotics on cancer chemotherapy, and will greatly benefit clinical practice in the treatment of cancers and the treatment of infectious diseases.

Abbreviations

COS: Cefotaxime sodium; CMS: Cefmetazole sodium; DDP: Cisplatin; 5-Fu: 5-fluorouracil; DMSO: Dimethlysulfoxide; FBS: Fetal Bovine Serum; NS: Neutral saline; NPC: Nasopharyngeal carcinoma; ROS: Reactive oxygen species; IR: Inhibition rate; OD: Optical density; TV: Tumor volume; RTV: Relative tumor volume; RPR: Relative proliferation rate of tumor;

Declarations

Acknowledgements

We thank Institute of Yunnan Tumor for friendly providing of all cell lines and research cooperation, Experimental Center for Medical Science Research of Kunming Medical University for help with flow cytometry, and Shanghai Qiming Biological Information LTD for help with microarray and RT-qPCR.

Authors' contributions

X.Q.H. designed the study, wrote the manuscript and performed data interpretation. X.Q.H., Q.Y., D.F., Y.T.Y. and L.D. performed in vitro anti-proliferation study. X.Q.H., Y.T.Y., W.J.L., L.D. and Z.P.Z. performed in vivo anticancer study in mice. X.Q.H., Y.T.Y., L.D. and Z.P.Z. performed FCM and Clone formation. Microarray assay and RT-qPCR were performed and analyzed by Shanghai Qi Ming Biological Information LTD. Q.Y. and Z.Y.S. helped with or advised on experiments and provided reagents. X.Q.H. performed statistical analysis.

Funding

This work was supported by grants to X.Q.H. from the National Natural Science Foundation of China (81760538), the Combination Foundation of Yunnan Provincial Science and Technology Department – Kunming Medical University (U0120170177), the Culture Grant of Great Science Achievements of Kunming Medical University (CGPY201603), and the Science and Technology Innovation Group Project of Yunnan Provincial Education Department.

Availability of data and materials

All data are available within the article and supplementary informations, or available from the author upon request. The raw microarray data files were submitted to Gene-Cloud of Biotechnology Information (GCBI) repository.

Ethics approval and consent to participate

Not applicable.

Consent for publication

All authors have agreed to the publication of this manuscript.

Competing interests

The authors declare that they have no competing interests.

Author details

[1]School of Public Health, Kunming Medical University, Kunming, Yunnan Province 650500, China.
[2]Institute of Yunnan Tumor, the Third Affiliated Hospital of Kunming Medical University, Kunming, Yunnan Province 650031, China.

References

1. Cantwell L, Perkins J. Infectious disease emergencies in oncology patients. Emerg Med Clin North Am. 2018; 36: 795-810.
2. Charshafian S, Liang SY. Rapid Fire: Infectious Disease Emergencies in Patients with Cancer. Emerg Med Clin North Am. 2018; 36: 493-516.
3. Chiang SK, Chen SE, Chang LC. A dual role of heme oxygenase-1 in cancer cells. Int J Mol Sci. 2018; 1: pii: E39. doi: 10.3390/ijms20010039.
4. Loboda A, Damulewicz M, Pyza E, Jozkowicz A, Dulak J. Role of Nrf2/HO-1 system in development, oxidative stress response and diseases: an evolutionarily conserved mechanism. Cell Mol Life Sci. 2016; 17: 3221-3247.
5. Nitti M, Piras S, Marinari UM, Moretta L, Pronzato MA, Furfaro AL. HO-1 Induction in Cancer Progression: A Matter of Cell Adaptation. Antioxidants. 2017; 2: 29.
6. Salerno L, Romeo G, Modica MN, Amata E, Sorrenti V, Barbagallo I, Pittalà V. Heme oxygenase-1: A new druggable target in the management of chronic and acute myeloid leukemia. Eur J Med Chem. 2017; 142: 163-178.
7. Chang LC, Fan CW, Tseng WK, Chein HP, Hsieh TY, Chen JR, Hwang CC, Hua CC. The Ratio of Hmox1/Nrf2 mRNA Level in the Tumor Tissue Is a Predictor of Distant Metastasis in Colorectal Cancer. Dis Markers. 2016; 2016: 8143465.
8. Chau LY. Heme oxygenase-1: emerging target of cancer J Biomed Sci. 2015; 22: 22.
9. Nemeth Z, Li M, Csizmadia E, Döme B, Johansson M, Persson JL, Seth P, Otterbein L, Wegiel B. Heme oxygenase-1 in macrophages controls prostate cancer Oncotarget. 2015; 32: 33675-33688.
10. Banerjee P, Basu A, Wegiel B, Otterbein LE, Mizumura K, Gasser M, Waaga-Gasser AM, Choi AM, Pal S. Heme oxygenase-1 promotes survival of renal cancer cells through modulation of apoptosis- and autophagy-regulating molecules. J Biol Chem. 2012; 287: 32113-32123.
11. Busserolles J, Megias J, Terencio MC, Alcaraz MJ. Heme oxygenase-1 inhibits apoptosis in Caco-2 cells via activation of AKT pathway. Int J Biochem Cell Biol. 2006; 38: 1510-1517.
12. Zhu XF, Li W, Ma JY, Shao N, Zhang YJ, Liu RM, Wu WB, Lin Y, Wang M. Knockdown of heme oxygenase-1 promotes apoptosis and autophagy and enhances the cytotoxicity of doxorubicin in

breast cancer cells. Oncology Letters. 2015; 10: 2974-2980.

13. Dixon SJ, Lemberg KM, Lamprecht MR, Skouta R, Zaitsev EM, Gleason CE, Patel DN, Bauer AJ, Cantley AM, Yang WS, et al. Ferroptosis: an iron-dependent form of nonapoptotic cell death. Cell. 2012; 5: 1060-1072.
14. Stockwell BR, Friedmann Angeli JP, Bayir H, Bush AI, Conrad M, Dixon SJ, Fulda S, Gascón S, Hatzios SK, Kagan VE, et al. Toyokuni, KA. Woerpel, DD. Zhang, Ferroptosis: A Regulated Cell Death Nexus Linking Metabolism, Redox Biology, and Disease. Cell. 2017; 2: 273-285.
15. Yang WS, SriRamaratnam R, Welsch ME, shimada K, Skouta R, Viswanathan VS, Cheah JH, Clemons PA, Shamji AF, Clish CB, et al. Regulation of Ferroptotic Cancer Cell Death by GPX4. Cell. 2014: 156: 317-331.
16. Chang LC, Chiang SK, Chen SE, Yu YL, Chou RH, Chang WC. Heme oxygenase-1 mediates BAY 11-7085 induced ferroptosis. Cancer Lett. 2018; 416: 124-137.
17. Hassannia B, Vandenabeele P, Vanden, Berghe T. Targeting Ferroptosis to Iron Out Cancer. Cancer Cell. 2019; 6: 830-849.
18. Waza AA, Hamid Z, Ali S, Bhat SA, Bhat MA. A review on heme oxygenase-1 induction: is it a necessary evil. Inflamm Res. 2018; 7: 579-588.
19. Kabir MF, Mohd Ali J, Haji Hashim O. Microarray gene expression profiling in colorectal (HCT116) and hepatocellular (HepG2) carcinoma cell lines treated with *Melicope ptelefolia* leaf extract reveals transcriptome profiles exhibiting anticancer activity. Peer J. 2018; 6: e5203.
20. Schmidt-Hieber M, Biewirth J, Buchheidt D, Cornely OA, Hentrich M, Maschmeyer G, Schalk E, Vehreschild JJ, Vehreschild Maria JGT, AGIHO Working Group. Diagnosis and management of gastrointestinal complications in adult cancer patients: 2017 updated evidence-based guidelines of the Infectious Diseases Working Party (AGIHO) of the German Society of Hematology and Medical Oncology (DGHO). Ann Hematol. 2018; 1: 31-49.
21. Vidal L, Paul M, Ben Dor I, Pokroy E, Soares-Weiser K, Leibovici L. Oral versus intravenous antibiotic treatment for febrile neutropenia in cancerpatients. Cochrane Database Syst Rev. 2013: 10: doi: 10.1002/14651858. CD003992.
22. Blanchard D. Prophylactic antibiotics to prevent surgical site infection after breast cancer Clin J Oncol Nurs. 2015; 19: 629-630.
23. De Silva N, Jackson J, Steer C. Infections, resistance patterns and antibiotic use in patients at a regional cancer Intern Med J. 2018; 48: 323-329.
24. Atzori A, Malloci G, Prajapati JD, Basciu A, Bosin A, Kleinekathofer U, Dreier J, Vargiu AV, Ruggerone P. Molecular interactions of cephalosporins with the deep binding pocket of the RND transporter AcrB. J Phys Chem B. 2019; 123: 4625-4635.
25. Drawz SM, Bonomo RA. Three decades of beta-lactamase Clin Microbiol Rev. 2010; 23: 160-201.
26. Weng TY, Wang CY, Hung YH, Chen WC, Chen YL, Lai MD. Differential Expression Pattern of THBS1 and THBS2 in Lung Cancer: Clinical Outcome and a Systematic-Analysis of Microarray Databases. PLoS One. 2016; 8: e0161007. doi: 10.1371/journal.pone.0161007.

27. Zhao J, Shi L, Zeng S, Ma C, Xu W, Zhang Z, Liu Q, Zhang P, Sun Y, Xu C. Importin-11 overexpression promotes the migration, invasion, and progression of bladder cancer associated with the deregulation of CDKN1A and THBS1. Urol Oncol. 2018; 6: 311.e1-311.e13.
28. Chen L, Wang G, Luo Y, Wang Y, Xie C, Jiang W, Xiao Y, Qian G, Wang X. Downregulation of LAPTM5 suppresses cell proliferation and viability inducing cell cycle arrest at G0/G1 phase of bladder cancer Int J Oncol. 2017; 1: 263-271.
29. Inoue J, Misawa A, Tanaka Y, Ichinose S, Sugino Y, Hosoi H, Sugimoto T, Imoto I, Inazawa J. Lysosomal-associated protein multispanning transmembrane 5 gene (LAPTM5) is associated with spontaneous regression of neuroblastomas. PloS One. 2009; 4: e7099.
30. Nuylan M, Kawano T, Inazawa J, Inoue J. Down-regulation of LAPTM5 in human cancer Oncotarget. 2016; 19: 28320-28328.
31. Narumi S, Hasegawa T. Association between SAMD9/SAMD9L and hematological malignancies. Rinsho Ketsueki. 2018; 11: 2475-2480.
32. Ma Q, Yu T, Ren YY, Gong T, Zhong DS. Overexpression of SAMD9 suppresses tumorigenesis and progression during non small cell lung cancer. Biochem Biophys Res Commun. 2014; 1: 157-161.
33. Wu L, Pu X, Wang Q, Cao J, Xu F, Xu LI, Li K. miR-96 induces cisplatin chemoresistance in non-small cell lung cancer cells by downregulating SAMD9. Oncol Lett. 2016; 2: 945-952.
34. Yokota T, Bui T, Liu Y, Yi M, Hunt KK, Keyomarsi K. Differential regulation of elafin in normal and tumor-derived mammary epithelial cells is mediated by CCAAT/enhancer binding protein beta. Cancer Res. 2007; 23: 11272-11283.
35. Hunt KK, Wingate H, Yokota T, Liu Y, Mills GB, Zhang F, Fang B, Su CH, Zhang M, Yi M, Keyomarsi K. Elafin, an inhibitor of elastase, is a prognostic indicator in breast cancer. Breast Cancer Res. 2013; 1: doi: 10.1186/bcr3374.
36. Caruso JA, Hunt KK, Keyomarsi K. The neutrophil elastase inhibitor elafin triggers rb-mediated growth arrest and caspase-dependent apoptosis in breast cancer. Cancer Res. 2010; 18: 7125-7136.
37. Yu KS, Lee Y, Kim CM, Park EC, Choi J, Lim DS, Chung YH, Koh SS. The protease inhibitor, elafin, induces p53-dependent apoptosis in human melanoma cells. Int J Cancer. 2010; 6: 1308-1320.
38. Shakhova I, Li Y, Yu F, Kaneko Y, Nakamura Y, Ohira M, Izumi H, Mae T, Varfolomeeva SR, Rumyantsev AG, Nakagawara A. PPP3CB contributes to poor prognosis through activating nuclear factor of activated T-cells signaling in neuroblastoma. Mol Carcinog. 2019; 3: 426-435.
39. Chen L, He Q, Liu Y, Wu Y, Ni D, Liu J, Hu Y, Gu Y, Xie Y, Zhou Q, Li Q. PPP3CB Inhibits migration of G401 cells via regulating epithelial-to-mesenchymal transition and promotes G401 cells growth. Int J Mol Sci. 2019; 2: doi: 10.3390/ijms20020275.
40. Van der Lelij P, Lieb S, Jude J, Wutz G, Santos CP, Falkenberg K, Schlattl A, Ban J, Schwentner R, Hoffmann T, et al. Synthetic lethality between the cohesin subunits *STAG1* and *STAG2* in diverse cancer Elife. 2017; 6: pii: e26980. doi: 10.7554/eLife.26980.
41. Benedetti L, Cereda M, Monteverde L, Desai N, Ciccarelli FD. Synthetic lethal interaction between the tumour suppressor STAG2 and its paralog STAG1. Oncotarget. 2017; 23: 37619-37632.

42. Ye XH, Huang DP, Luo RC. NCOA5 is correlated with progression and prognosis in luminal breast cancer. Biochem Biophys Res Commun. 2017; 2: 253-256.
43. Sun K, Wang S, He J, Xie Y, He Y, Wang Z, Qin L. NCOA5 promotes proliferation, migration and invasion of colorectal cancer cells via activation of PI3K/AKT pathway. Oncotarget. 2017; 4: 107932-107946.
44. Trachootham D, Alexandre J, Huang P. Targeting cancer cells by ROS-mediated mechanisms: A radical therapeutic approach? Nat Rev Drug Discov. 2009; 8: 579-591.
45. Liou GY, Storz P. Reactive oxygen species in cancer. Free Radic Res. 2014; 44: 1-5.
46. Cui Q, Wang JQ, Assaraf YG, Ren L, Gupta P, Wei L, Ashby CR Jr, Yang DH, Chen ZS. Modulating ROS to overcome multidrug resistance in cancer. Drug Resist Updat. 2018; 41: 1-25.

Figures

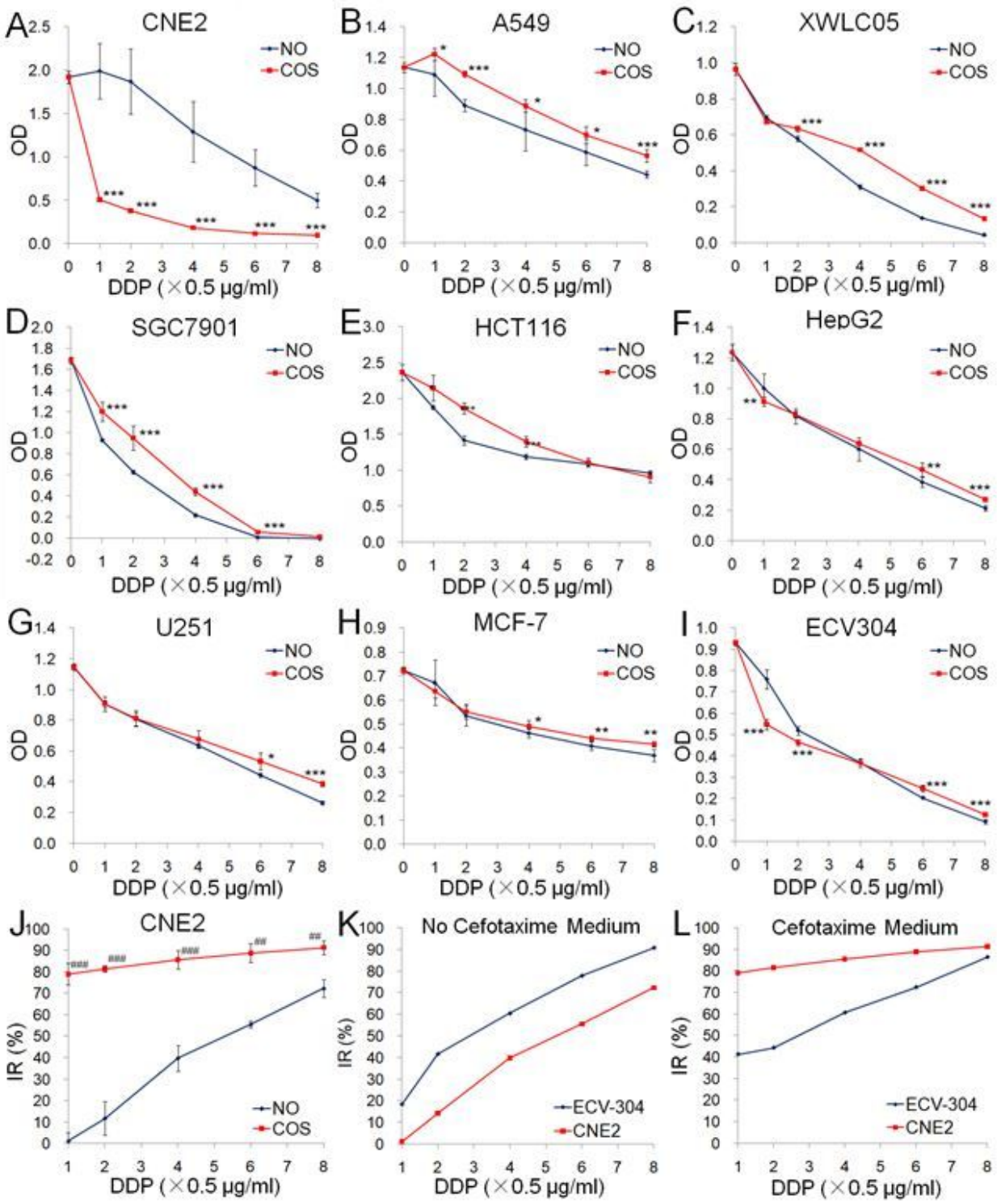

Figure 1

Cell viability in different cell lines treated with DDP in COS medium (COS) or no COS medium (NO). A-I OD values in CNE2, A549, XWLC05, SGC7901, HCT116, HepG2, U251, MCF7 and ECV304 cells in DDP group (NO) and COS+DDP group (COS), respectively. Data are presented as mean ± SD. Error bars represent SD from six replicates. *p < 0.05, **p < 0.01, ***p < 0.001 denote significant differences. J Comparison of the inhibition rates of cell viability (IR) in CNE2 cells between DDP group (NO) and COS+DDP group (COS).

Error bars represent SD from three replicates. #p < 0.05, ##p < 0.01, ###p < 0.001 denote significant differences. K IR in CNE2 and ECV-304 treated with DDP in no cefotaxime medium (NO). L IR in CNE2 and ECV-304 treated with DDP in cefotaxime medium (COS). IR: Percentage inhibition rate of cell viability.

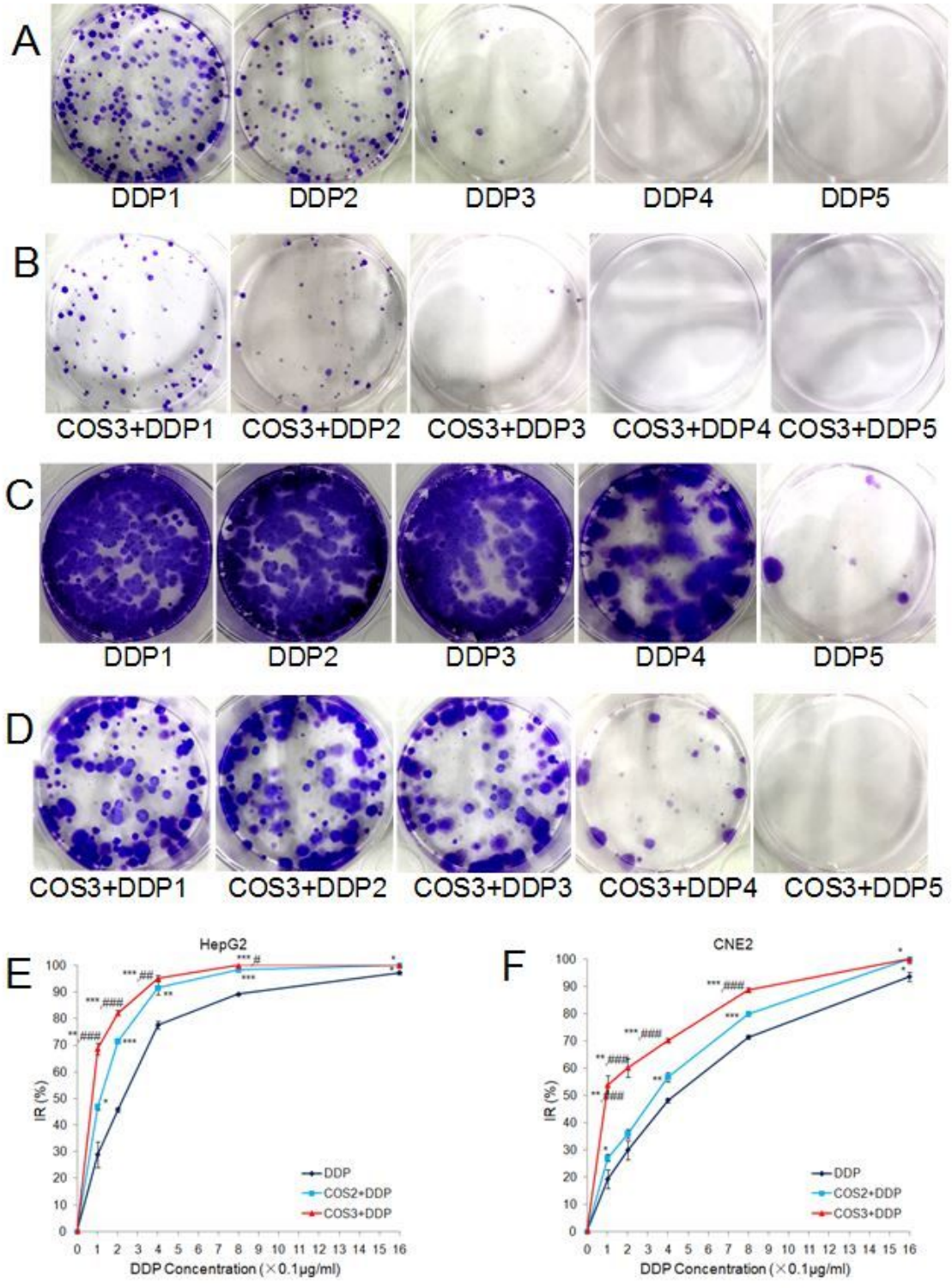

Figure 2

COS decreases clone formation of cancer cells treated by DDP. A Photos of clone in HepG2 treated by DDP in no cefotaxime medium. B Photos of clone in HepG2 treated by DDP in cefotaxime medium (100

μg/ml). C Photos of clone in CNE2 treated by DDP in no cefotaxime COS medium. D Photos of clone in CNE2 treated by DDP in cefotaxime medium (100 μg/ml). E Inhibition rates of clone formation (IR) in HepG2. Error bars represent SD from three replicates. */#p < 0.05, **/##p < 0.01, ***/###p < 0.001 denote significant differences. F Inhibition rates of clone formation (IR) in CNE2. Error bars represent SEM from three replicates. */#P < 0.05, **/##P < 0.01, ***/###P < 0.001 denote significant differences. *: IR comparison between COS2+DDP group (and COS3+DDP group) and DDP group. #: IR comparison between COS3+DDP group and COS2+DDP group. IR: Percentage inhibition rate of clone formation.

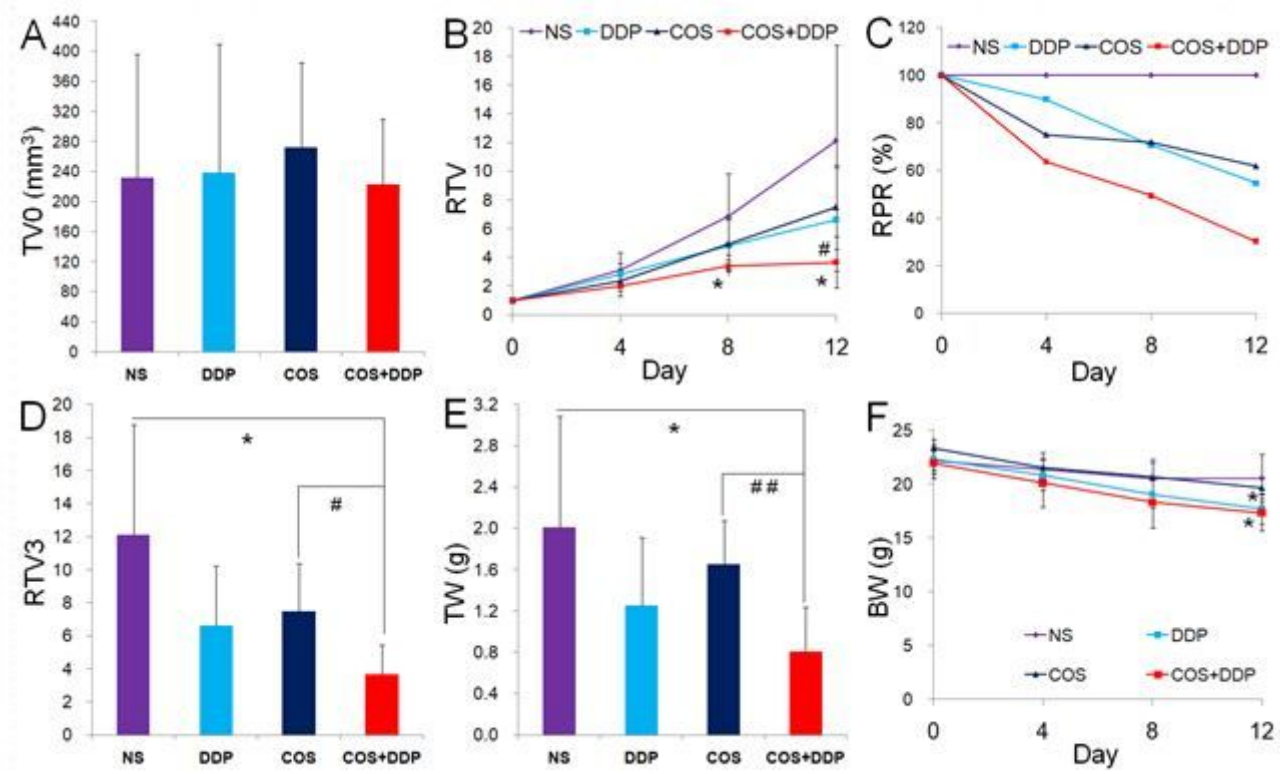

Figure 3

Cefotaxime enhances the anticancer efficacy of DDP in NPC xenograft mouse model. A Original tumor volume (TV0) in each group before drug administration. B Relative tumor volume (RTV) in each group throughout the study. C Relative proliferation rate (RPR) of tumor in each group throughout the study. D RTV3 (RTV at the end of the study) comparison among different groups. E TW (Tumor weight at the end of the study) comparison among different groups. F Body weight (BW) in each group throughout the study. Error bars represent SD from six mice. */#P < 0.05, **/##P < 0.01 denote significant differences. *: Comparison between combination group and NS control group. #: Comparison between combination group and COS group.

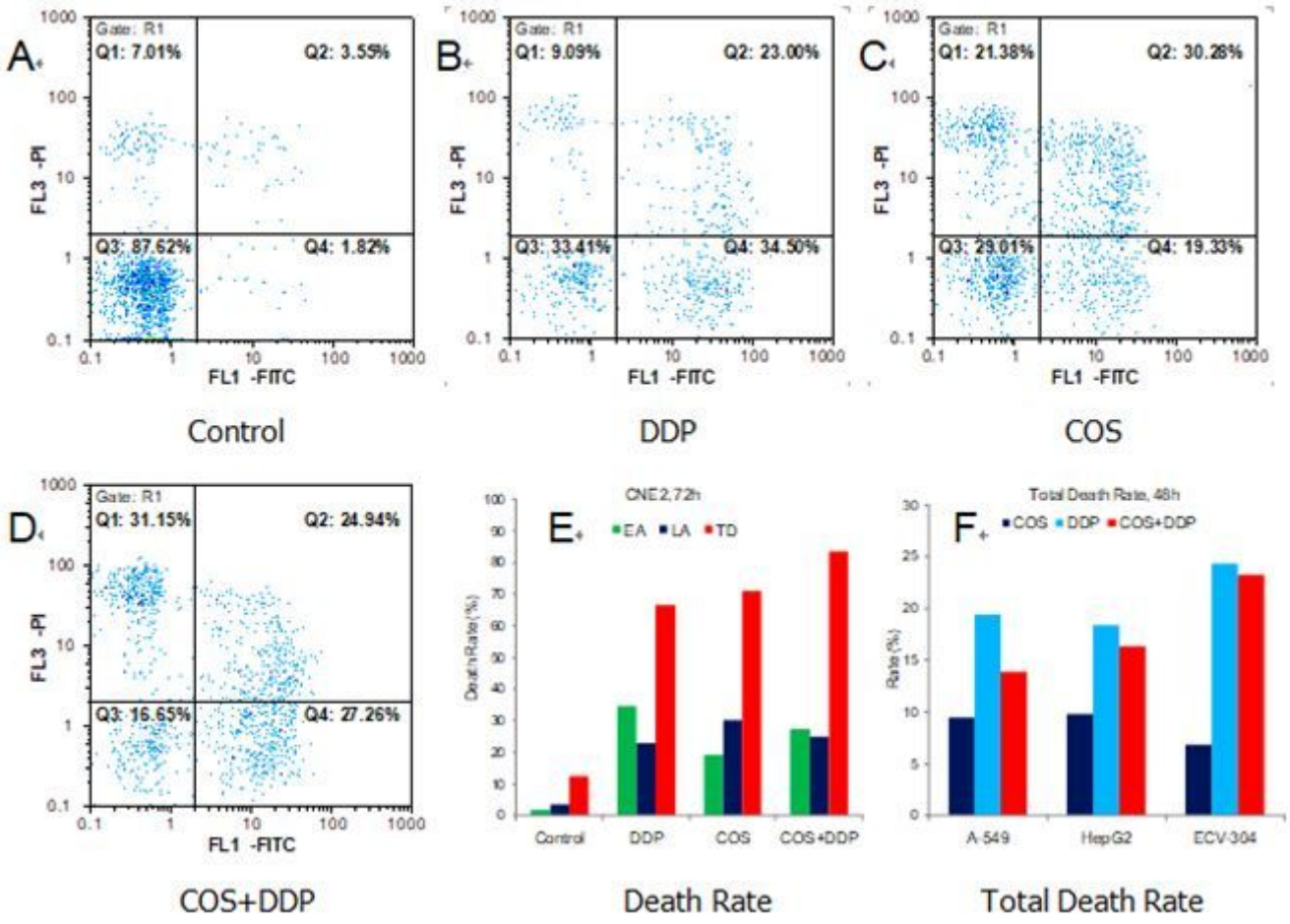

Figure 4

Apoptosis induced by COS, DDP and COS+DDP. A Photo of apoptosis in negative control group in CNE2. B Photo of apoptosis in DDP group in CNE2. C Photo of apoptosis in COS group in CNE2. D Photos of apoptosis in COS+DDP group in CNE2. E Quantification of apoptosis distribution in CNE2 at 72h. F Quantification of apoptosis distribution in other cell lines at 48h.

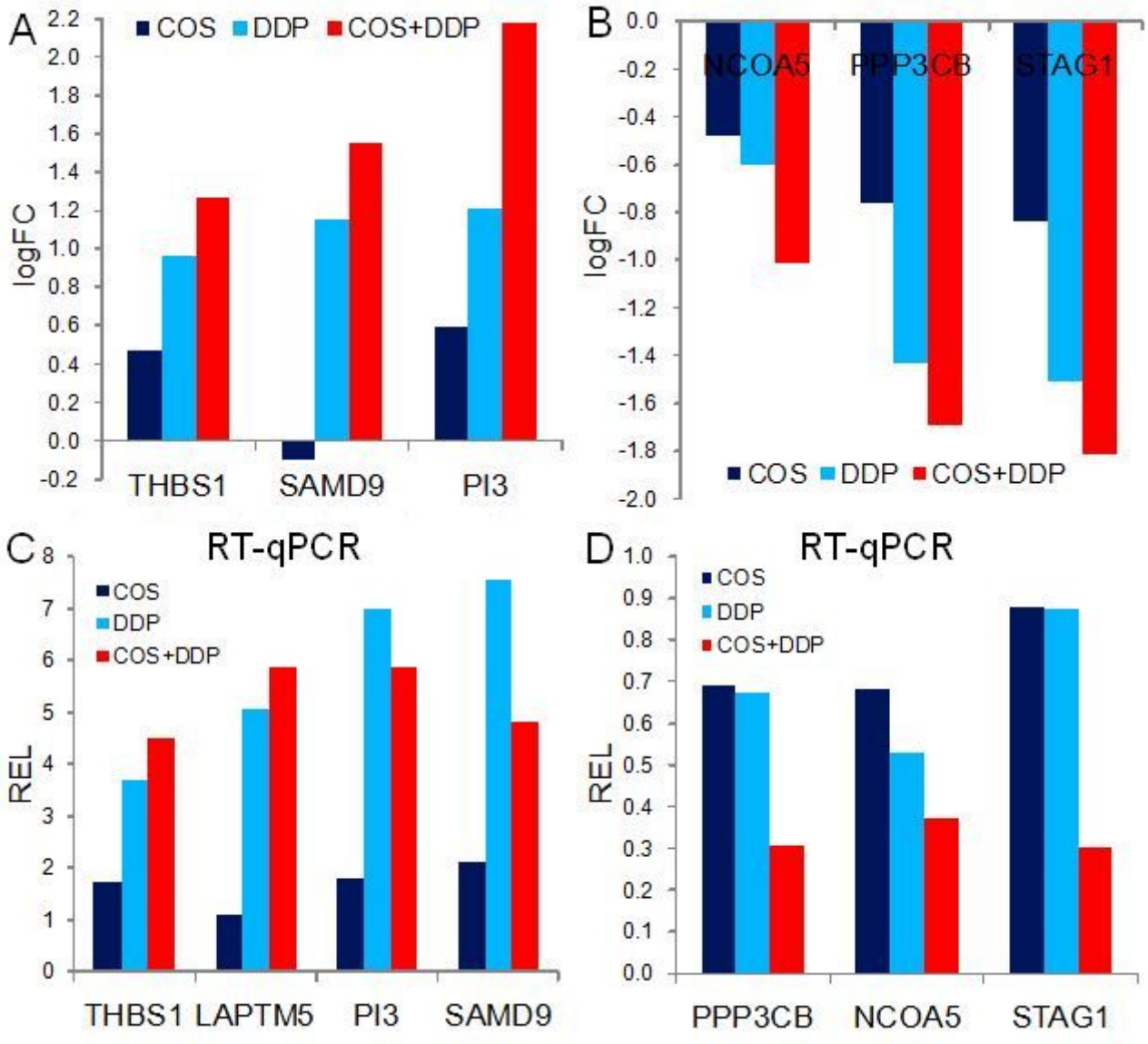

Figure 5

Expression levels of differential coding genes favoring anticancer efficacy in combination group. A LogFC of the jointly upregulated genes by microarray. B LogFC of the jointly downregulated genes by microarray. C Relative expression level (REL) of the upregulated genes validated by RT-qPCR. D Relative expression level (REL) of the downregulated genes validated by RT-qPCR.

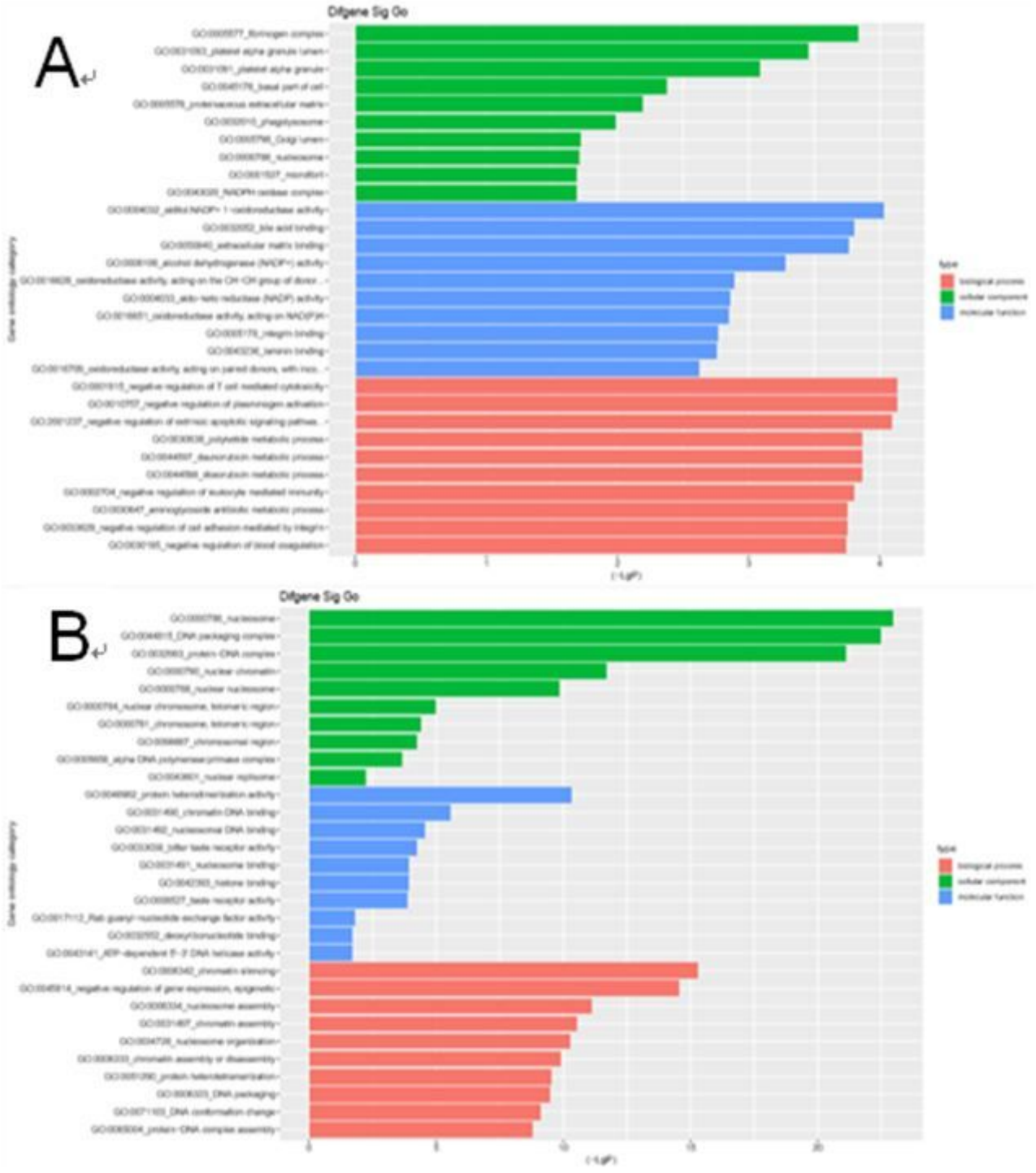

Figure 6

The top ten biological processes, cell components and molecular functions (GO-term) significantly regulated in combination group. A Upgene-Sig-Go in CNE2 cells in combination group. B Downgene-Sig-Go in CNE2 cells in combination group.

Supplementary Files

This is a list of supplementary files associated with this preprint. Click to download.

- SupplementryTabless1tos5.docx
- Supplementryfigures1.docx